

Integrative Analysis of Gene Expression and DNA Methylation Depicts the Impact of Obesity on Breast Cancer

zhenchong xiong

Sun Yat-sen University Cancer Center <https://orcid.org/0000-0002-1129-5663>

Lin Yang

Southern Medical University Nanfang Hospital

Jianchang Fu

Sun Yat-sen University Cancer Center

Xing Li

Sun Yat-sen University Cancer Center

Xinhua Xie

Sun Yat-sen University Cancer Center

Yanan Kong

Sun Yat-sen University Cancer Center

Xiaoming Xie (✉ xiexm@sysucc.org.cn)

Sun Yat-sen University Cancer Center

Research article

Keywords: Obesity, breast cancer, adipose cell, immune, immune checkpoint inhibitor, DNA methylation

Posted Date: December 1st, 2020

DOI: <https://doi.org/10.21203/rs.3.rs-113914/v1>

License:   This work is licensed under a Creative Commons Attribution 4.0 International License.

[Read Full License](#)

Abstract

Background: Obesity has been reported to be a risk factor for breast cancer, but how obesity affects BC is unclear. Although BMI is the most commonly used marker for obesity, it is insufficient to evaluate the obesity-related pathophysiological changes in breast tissue. The purpose of this study was to establish a DNA-methylation-based biomarker for obesity and to explore the association of obesity with BC.

Methods: Lasso regression was used to develop DNA-methylation-based BMI index (DM-BMI). Linear regression and paired t-test were used to assess the accuracy of DM-BMI in BMI prediction. A deconvolution algorithm based on DNA methylation data was used to calculate the proportion of adipose cell in tissues. The Estimate and Cibersort algorithm were used to assess the degree of tumor-infiltrating immune cells.

Results: Using DNA methylation data from TCGA and GEO, we developed DM-BMI to evaluate the degree of obesity in breast tissues. In tissues from non-BC and BC population, the DM-BMI model exhibited high accuracy in BMI prediction. In BC tissues, DM-BMI correlated with increased adipose tissue content and BC tissues with increased DM-BMI exhibited higher expression of pro-inflammatory adipokines. Next, we identified the gene expression profile relating to DM-BMI. Using GO and KEGG database, we observed that the DM-BMI-related genes mostly involve in the process of cancer immunity. DM-BMI is positively correlated with T cell infiltration in BC tissues. Further, we observed that DM-BMI positively correlated with immune checkpoint inhibitors [1] response markers in BC.

Conclusions: Collectively, we developed a new biomarker for obesity and discovered that BC tissues from obese individuals exhibit an increased degree of immune cell infiltration indicating that obese BC patients might be the potential beneficiaries for ICI treatment.

Background

Breast cancer is the most commonly diagnosed cancer and the second leading cause of cancer death for women in the world [2]. Previous study has reported that obesity, which is characterized by excess adipose tissues, is a risk factor for BC [3]. In premenopausal women, obesity associated with increased risk of hormone receptor (HR) negative BC. In postmenopausal women, obesity associated with increased risk of HR positive BC [4]. Moreover, several studies showed that obese patients exhibited more aggressive tumor features (such as larger tumor size, lymph node metastasis, shorter disease-free survival and greater risk of mortality) comparing to non-obese patients in BC [5, 6]. Although previous studies have observed that the adipose tissue in obese individuals increasingly secretes adipokines (including hormones, growth factors, and cytokines) contributing to an environment promoting cancer proliferation and metastasis[7], how obesity impacts BC requires further studies.

Body Mass Index (BMI), which is defined as a person's weight in kilograms divided by the square of height in meters, is the most commonly used method for obesity evaluation. However, it is more like a surrogate measure for body fatness while obesity should be calculated using the excess accumulation of

adipose tissues rather than body mass [8]. As heterogeneity exists in the body distribution, function and tissue composition of adipose tissue among BC patients, a total body mass index is insufficient to evaluate the degree of obesity in local tissue. Moreover, BMI could only reflect the gain of weight but not to reflect the pathophysiological changes during the process of obesity [9]. Thus, developing new biomarkers to evaluate the obesity status of BC tissues is helpful to assess the impact of obesity on BC.

It is well known that obesity is affected by multiple factors (including environmental factors, genetic predisposition and the individual lifestyle) [10]. Recently, an increasing body of evidences showed that DNA methylation also involved in the process of obesity [11, 12]. DNA methylation is an epigenetic mechanism which regulates gene expression through chromatin structure changes. Equally influenced by environmental factors, genetic predisposition and the individual lifestyle, the level of gene methylation is dynamically changing setting up stable gene expression profiles to adapt the process of obesity. Study analysing the whole genome methylation and gene expression in non-diseased breast showed that obesity associated with the genome-wide methylation changes in human tissue [13]. In addition, Brionna Y Hair et al. observed that obesity significantly associated with genome-wide hyper-methylation in ER-positive BCs [14]. Thus, changes of genome-wide DNA methylation could be a reflection of the biological changes in breast tissue during the process of obesity. The goal of our study is to capture the obesity-related genomic changes and to explore the impact of obesity on BC tissues. We developed DNA methylation based BMI index (DM-BMI) to evaluate the degree of obesity in breast tissues. We validated the accuracy of DM-BMI in breast tissues from non-BC and BC population. Further, we assessed the correlation of DM-BMI with the obesity adipose tissue content and with the expression of adipokines in BC tissues. Next, we identified the DM-BMI related gene expression profile. Using Gene Ontology (GO) and Kyoto Encyclopedia of Genes and Genomes (KEGG) database, we observed that the DM-BMI-related genes significantly involved in the process of cancer immunity. Using Estimate and Cibersort algorithm, we observed a positive correlation between DM-BMI and immune cell infiltration. Finally, we assessed the correlation between DM-BMI and biomarkers of response to immune checkpoint inhibitors [1] and observed that DM-BMI positively correlated with ICI response in BC.

Methods

Data collection and processing

The training set including the genome-wide methylation data of 221 normal breast tissues in GEO (GSE88883 and GSE101961) and the validation sets including data of 44 normal breast tissues (the validation set 1) and data of 70 tumor-adjacent breast tissues (the validation set 2) in GEO (GSE67919 and GSE74214) were used to developed the DM-BMI score. The BMI data of the above cases were listed in Suppelmentary materials 1–2. The DNA methylation and expression data of 76 cases with matched tumor and tumor-adjacent breast tissues and the data of 699 cases with unmatched tumor tissues were collected from The Cancer Genome Atlas (TCGA) database.

Genome-wide methylation data was profiled using Illumina Infinium HumanMethylation450 BeadChips Assay. For DNA methylation data, β value ranging from 0 (no DNA methylation) to 1 (complete DNA methylation) was used to define the methylation level of each probe, and the probes with missing value in over 50% samples were removed while the probes with missing value in less than 50% samples were imputed with the k-nearest neighbors (knn) imputation method. Probes located on the sex chromosome and probes containing known single nucleotide polymorphisms (SNPs) were removed. Eventually, 301998 probes were included in this study. BMIQ normalization for type I and II probe correction was performed. Data from multiple studies was integrated and the Combat algorithm was performed to remove the batch effects. The above processes were carried out using the R package Champ.

For gene expression data, background correction and normalization were carried out using the R package limma.

Calculation of DNA-methylation based BMI index

To improve the predictive accuracy of the model, the BMI value was transformed to F(BMI) before further analysis as follow:

$$F(\text{BMI}) = \log(\text{BMI} + 1) - \log(\text{healthy.BMI} + 1) \text{ if } \text{BMI} \leq \text{healthy.BMI};$$
$$F(\text{BMI}) = (\text{BMI} - \text{healthy.BMI}) / (\text{healthy.BMI} + 1) \text{ if } \text{BMI} > \text{healthy.BMI}.$$

The parameter healthy.BMI was set to 25 referring to the upper limit of BMI in healthy population.

A lasso regression was used to regress the DM-BMI in the form of F(BMI) based on the BMI data and DNA methylation Data with 301998 probes. 42 probes was selected in the lasso regression model as BMI predictors according to the lambda.min value (Fig. S1A), and the coefficient values of each probe was shown in Fig. S1B. The lasso regression analysis was carried out using the R package glmnet (alpha was set to 1, and the lambda value was identified by performing a 10-fold cross validation to the training data).

Analysis of intra-sample adipose tissue content

Adipose tissue accounts for a large proportion of breast tissue composition. We used a deconvolution algorithm to calculate the proportion of adipose tissue in breast and BC tissues based on DNA methylation. Andrew E. et al provided a deconvolution algorithm to model cell subpopulations in breast tissues based on DNA methylation data. Illumina 450 k DNA methylation data of human mammary epithelial cells (GSE40699) and adipose tissue (GSE48472) were used as reference profiles. Data was processed as previous description, and probes which have an absolute difference in beta-value between the human mammary epithelial cells and the averaged adipose tissue > 0.7 were selected for the evaluation of intra-sample adipose tissue content. Data of adipose tissue content were listed in Supplementary material 3.

Characteristics analyses of BMI predictors

42 probes were selected in the lasso regression model as BMI predictors. The distribution of 42 probes on chromosome, CpG island, TSS regions was assessed using the R package Champ. BMI predictors which were differentially methylated between BC tissues and tumor-adjacent breast tissues in TCGA database were identified using the R package Champ. The survival correlation of BMI predictors was assessed using TCGA BRCA data. Correlation between the methylation level of BMI predictors and DM-BMI was assessed.

Functional and clinical characteristics analysis of DM-BMI related gene profile

DM-BMI of TCGA-BC tissues were calculated using DNA methylation data, and Spearman correlation coefficient was used to assess the correlation of DM-BMI and clinical characteristics (menopause status, hormone status, copy number variation and gene mutation) in BC. Gene expression profile related to DM-BMI was identified, and functional analysis of the related genes were processed by GO and KEGG analysis. Otherwise, we performed Gene set variation analysis (GSVA) analysis to identify DM-BMI related gene signature using gene expression data in TCGA. The above procedure were performed using the R software.

Evaluation of correlations between DM-BMI and the immune microenvironment in BC.

Tumor mutation burden (TMB) was defined as the number of non-synonymous mutations/Mb of genome. As previously reported [15], TMB of BC tissues in TCGA was calculated as (whole exome non-synonymous mutations)/38 (Mb).

The level of tumor-infiltrating immune cells and stromal cells in each tissue were evaluated by ESTIMATE algorithm [16]. The proportion of 22 immune cells in each tissue were evaluated by CIBERSORT algorithm (<http://cibersort.stanford.edu/>) [17]. Correlations between DM-BMI and ESTIMATE/ CIBERSORT scores were calculated using Spearman correlation coefficient. The data of TMB, ESTIMATE and CIBERSORT analysis were listed in Supplementary material 4.

Evaluation of correlations between DM-BMI and the cancer immunotherapy response.

The following biomarkers were used to predict the immunotherapy response: IFN- γ signature (IFNG) [18], IFNG hallmark gene set (IFNG.GS) [19], antigen processing and presenting machinery (APM) score [20], CD274, CD8, Tumor Immune Dysfunction and Exclusion (TIDE) [21], myeloid-derived suppressor cells (MDSCs), cancer-associated fibroblasts (CAFs) and the M2 subtype of tumor-associated macrophages (TAM-M2) [22]. IFNG was calculated by averaging of 6 genes (IFNG, STAT1, IDO1, CXCL9, CXCL10, HLA-DRA). IFNG.GS was calculated as the average expression of all genes in the set. APS was defined as the mRNA expression status of APM genes (PSMB5, PSMB6, PSMB7, PSMB8, PSMB9, PSMB10, TAP1, TAP2, ERAP1, ERAP2, CANX, CALR, PDIA3, TAPBP, B2M, HLA-A, HLA-B and HLA-C). CD274, CD8, TIDE, MDSCs, CAFs and TAM-M2 were calculated using the web application (<http://tide.dfci.harvard.edu>). The relevant data were listed in Supplementary material 4.

Results

Development and validation of DM-BMI in breast, tumor-adjacent and BC tissues.

A total of 221 breast tissues from non-BC cases (GEO database) were selected as the training cohort to develop the DNA-methylation-based BMI (DM-BMI) prediction model (Fig. 1). The median BMI and median age of training cohort were 28.24 (6.07–53.74) and 37 (17–82). 50 lasso regression models based on DNA methylation data of training cohort (301998 probes per sample) were constructed and the model with the minimum mean-squared error was selected based on the Lambda value (Fig.S1A). 42 probes were included and the coefficients of them were shown in Fig.S1B and Supplementary material 5. We used Spearman correlation coefficient and paired t-test to assess the predictive accuracy of the DM-BMI model. DM-BMI showed a significant correlation with BMI (Fig. 2A) and paired t-test revealed that there was no significant difference between DM-BMI and BMI ($t = -0.384$, $df = 220$, $p\text{-value} = 0.702$). Using a deconvolution algorithm, we evaluated the breast tissue composition and observed that the increased DM-BMI was significantly correlated with higher proportion of adipose tissue (Fig. 2B). These results showed the high accuracy of DM-BMI for BMI prediction.

Next, 44 normal breast cases (validation set 1) and 70 tumor-adjacent breast tissues (validation set 2) were enrolled for external validation (Fig. 1). The median BMI and median age of validation set 1 were 27.1 (14.6–62.7) and 44 (13–80). The median BMI and median age of validation set 2 were 28.65 (16.5–53.4) and 56 (29–84). Both in validation set 1 and 2, DM-BMI showed positive correlation with BMI (Fig. 2C and 2E) and paired t-test revealed that there was no significant difference between DM-BMI and BMI ($t = -0.253$, $df = 43$, $p\text{-value} = 0.801$, validation set 1; $t = -1.87$, $df = 69$, $p\text{-value} = 0.066$, validation set 2). Moreover, DM-BMI significantly correlated with adipose tissue proportion in both normal and tumor-adjacent breast tissues (Fig. 2D and 2F). The above results showed a high prediction accuracy of DM-BMI model in both normal and tumor-adjacent breast tissues.

Further, we assessed the DM-BMI of paired tumor and tumor-adjacent breast tissues in TCGA database. The tumor tissues exhibited a higher level of DM-BMI comparing to its paired tumor-adjacent tissues (Fig. 2G). In BC tissues, DM-BMI positively correlated with adipose tissue proportion (Fig. 2H).

What Is Known About The 42 Bmi Predictors?

As DM-BMI was significantly correlated with the obesity status which has been suggested to risk factor for BC, we further assessed the relevance between BMI predictors and BC. As hyper-methylation of CpG Island at gene promoter regions often caused gene silencing, we first evaluated the distribution of BMI predictors. Among 22 pairs Chromosome (Chr), Chr1 and 16 are the most common region for BMI predictor distribution. 45.2% of BMI predictors located at the gene body regions while only 23.8% of them located at the promoter regions (TS1500 and TS200). Further, we observed that only a few part of BMI predictors located at CpG islands (Fig. 3A).

Next, we assessed the methylation variation of BMI predictors between tumor and tumor-adjacent breast tissues. 26 differentially methylated probes (DMP) were identified: 22 BMI predictors were hyper-methylated in tumor tissues comparing to the tumor-adjacent breast tissues and 4 were hypo-methylated in tumor (Fig. 3B). 3 of 42 BMI predictors correlated better OS for BC patients and 2 of them were located at gene-coding regions (Fig. 3C). In BC tissues, the correlation between methylation level of 42 BMI predictor and DM-BMI were evaluated and 11 of them significantly correlated with DM-BMI (correlation coefficient > 0.3 or < -0.3 ; Fig. 3D-E). By integrative analysis of DNA methylation and expression data, the negatively correlation between methylation level and gene expression were observed in 22/42 BMI predictors (Fig. 3E).

Functional and clinical characteristics analysis of DM-BMI related gene profile in BC.

Further, we explored the biological significance of DM-BMI in breast cancer tissues. The survival correlation of DM-BMI was evaluated in BCs and subgroup of BCs with cancer therapy (chemotherapy, endocrine-therapy, anti-HER2 therapy and radiation-therapy). DM-BMI was consistently correlated with higher mortality risk in the whole cohort of BC patients and subgroups of patients with chemotherapy, endocrine-therapy or radiation-therapy, respectively (Table 1). Tissues from patients with postmenopausal status and TP53-mutation exhibited a significantly higher level of DM-BMI (Fig. 4A-B). Otherwise, an increasing level of DM-BMI was correlated with increased proportion of ERBB2 and MYC amplification (Fig. 4C-D).

Table 1. Survival analysis of DM-BMI in BC with systemic therapy			
Subgroup	HR (High vs Low)	95%CI	P value
Overall	1.046329459	1.005-1.089	0.027924058
Chemotherapy	1.100065801	1.029-1.176	0.00529122
Hormone therapy	1.087123098	1.009-1.171	0.027857745
Anti-HER2 therapy	1.048120675	0.832-1.320	0.689677033
Radiation therapy	1.0775886	1.003-1.158	0.041331982

Previous studies showed that adipokines produced by obese adipose tissues drives obesity-mediated inflammation and BC progression. In BC tissues, proportion of adipose tissue was positively correlated with DM-BMI. Expression of 6 pro-inflammatory adipokines were positively correlated DM-BMI while expression of 2 anti-inflammatory adipokines were negatively correlated DM-BMI (Fig. 4E). These results indicated that obesity increased the expression of pro-inflammatory adipokines in BC tissues.

Further, we assessed the DM-BMI (obesity) related gene expression profile and mRNA expression of 10032 gene significantly correlated with DM-BMI. To evaluate the biological effect of obesity on BC, we performed GSEA analysis of DM-BMI related genes using KEGG and GO database. GO analysis showed

that genes positively correlated with DM-BMI were significantly involved in antigen processing and presentation, immune cell activation, MHC protein binding, immune receptor activity in BC (Fig. 4F). KEGG consistently showed that DM-BMI related genes were significantly enriched in tumor-immunity related pathway (including: antigen processing and presentation, NK cell mediated cytotoxicity, T cell differentiation, and PD-1 checkpoint pathway) (Fig. 4G). These results indicated that the obesity-related gene profile involved in the regulation of immune response in BC.

DM-BMI correlated with T cell infiltration and ICI response markers in BC.

We evaluated the correlation between obesity and immune response to BC. Gene mutation which changes protein-coding sequence and leads to the expression of abnormal proteins was suggested to be the driving factor for cancer development. Also, the abnormal protein derived from tumor mutation might arise immune response. In BC tissues, we observed a positive correlation between DM-BMI and TMB. Using Estimate algorithm, we evaluated the degree of immune cell infiltration in TCGA BC tissues. Interestingly, we found a positive correlation between DM-BMI and Estimate-immune score while no significant correlation was observed between DM-BMI and Estimate-Stromal score (Fig. 5B). Next, we calculated the relative abundance of 22 immune cell types in TCGA BC tissues. Among them, the content of CD8-T, CD4 memory activated-T, T follicular helper and regulatory T cells (Treg) were positively correlated with DM-BMI indicating the more intense T cell mediated immune response in BC tissues with increased DM-BMI (Fig. 5C). As the representative of immunotherapy, the ICI therapy suppressed BC progression by activating T cell mediated immune response. Thus, we examined whether DM-BMI predicted the tumor response to ICI. 5 markers for ICI response and 4 markers for ICI resistance were selected to evaluate the tumor response. In BC tissues, DM-BMI positively correlated with IFNG, IFNG.GS, CD274, CD8 and APS indicating that BC tissues with increased DM-BMI exhibited a better response to ICI (Fig. 5D). Moreover, DM-BMI was negatively correlated with two ICI resistance markers (CAFs and TAM-M2). All these results indicated that BC tissue at obesity status might exhibit a more intense response to ICI based on markers of ICI response.

Discussion

In this study, we developed an obesity evaluation model (DM-BMI) based on DNA methylation pattern. Based on the DM-BMI model, we further identified the obesity-related gene expression profile. Although obesity has been shown to be a BC risk factor for many years, most studies focus on the correlation between obesity and clinical prognosis while studies about the biological and genomic impact of obesity on breast cancer were limited. The adipose tissue, as the major agent mediating obesity-related biological effects, is an important starting point for the study of the obesity impact. In both breast and BC tissue, we observed a positive correlation between the proportion adipose tissue content and DM-BMI. Previous study reported that the expansion of adipose tissue, accompanied by the dys-regulation of the endocrine function (adipokine secretion) of the adipose cells, was driven by an increase in size of adipose or by

formation of new adipose cell. As the DM-BMI increased, we observed an increased expression of pro-inflammatory adipokines and decreased expression of anti-inflammatory adipokines which might synergistically induce obesity-mediated inflammation through activation of NF- κ B pathway and create a pro-oncogenic environment.

In addition to the expansion of adipose tissue, we also observed a promoting effect of obesity on immune response in BC tissue. In obese individuals, adipose tissue expands with increasing demand of oxygen which induces the development of a hypoxia environment. The activation of hypoxia signaling increases the expression of adipokines, especially the pro-inflammatory adipokines (including CCL2, CXCL8, CXCL10, IL-18, IL-1 α and Oncostatin M) which involve in the recruitment of tumor-associated immune cells. Moreover, previous study also showed that adipocytes could fuel immune cells through releasing exosome-sized, lipid-filled vesicles [23]. In BC tissues, we observed that DM-BMI positively correlated with the degree of M1 macrophages, activated dendritic cell and T cell infiltration indicating an increase activity of tumor immune response. As T cell exhaustion is critical for tumor immune escape, previous study indicated that T cell exhaustion could be reversed by immune checkpoint inhibition (such as PD-1) and replenishing activated T cells (such as CAR-T). Interestingly, in obese BC tissues, we found an increase content of CD4⁺, CD8⁺ and follicular helper T cells, which may be due to the increased secretion of immune chemokines in adipose tissue. Although we also observed a positive correlation between DM-BMI and regulatory T cell (Treg), a subset of immune cell with immunosuppressive activity, it can be interpreted as a negative feedback regulation by the immune system to maintain the stability of the immune environment after the activation of the immune response [24]. Further, our study revealed that DM-BMI positively correlated with ICI response markers in BC tissues. These results suggest that obese BC patients may benefit from ICI. Recently, Wang, Z. et al consistently reported that obesity is associated with increased response of PD-1/PD-L1 blockade in animal melanoma tumors model [25]. However, as our findings were mainly supported by database analysis, data from clinical samples treated with ICI treatment are still required to validate the correlation between DM-BMI and ICI response.

With the increasing number of obese patients, the impact of obesity on the treatment of breast cancer has attracted more and more attention. We observed that increased DM-BMI was correlated with higher mortality risk in patients with chemotherapy, hormone-therapy and radiation-therapy. Although no evidence pointed out that obesity induces drug-resistance in cancer cell, dose of chemotherapy and radiation might be routinely reduced in obese individuals because doctors usually limit body surface area under 2 m² to reduce toxicity when calculating the dose of chemotherapy [4, 26]. As highly expression of aromatase, adipose tissue is an endocrine organ which is an important site for estrogen biosynthesis, especially in postmenopausal women [27]. In obese BC patients, increased expression of aromatase might cause the resistance to endocrine-therapy.

Because of the limitation of BMI in obesity evaluation, several imaging methods have been developed for obesity evaluation (including: bioimpedance analysis instruments, dual-energy X-ray absorptiometry, computed tomography and magnetic resonance imaging) [28, 29]. Although these newly methods enable the precise quantification of adipose tissue, the operational complexity has limited their application [30].

Developing new methods to evaluate the degree of obesity is of great value. Recently, increasing number of studies indicated that environmental factors (such as dietary pattern and life style) induce changes in DNA methylation pattern predisposing to obesity and obesity, likewise, results in genome-wide methylation variation [11, 31]. Moreover, biomarkers based on DNA methylation have been shown to be effective in obesity evaluation while most of them were only applied in blood samples [11]. Thus, we developed a DNA-methylation-based biomarker (DM-BMI) for obesity evaluation in breast tissue. In both normal breast and tumor-adjacent breast tissue, DM-BMI showed a significant correlation with both BMI and the content of adipose tissue. In addition, we also observed that DM-BMI was positively correlated with the degree of pro-inflammatory adipokines and immune cells infiltration in BC tissues. All these data indicated that DM-BMI is an effective biomarkers to evaluated the biological changes in tumor tissues of obese patients.

The identification of BMI predictors naturally cause the assumption that whether these CpGs are critical regulators of obesity. In our study, only 11 of 42 BMI predictors significantly correlated with DM-BMI while the others exhibited negligible correlation with DM-BMI. Although DNA methylation level were negatively correlated with gene expression in over half of BMI predictors, 45.2% of BMI predictors located at the body region of gene sequence. How CpGs located at body region regulate gene expression is unclear. As previous study reported that variations of DNA methylation pattern are the consequence of adiposity rather than the cause [31], whether these BMI predictors are regulators of obesity or the imprints of the biological process needs further investigation.

Conclusion

Collectively, we established a new biomarker for obesity evaluation and discovered that BC tissues of obese individuals exhibit an increased degree of immune cell infiltration indicating that obese BC patients might be the potential beneficiaries for ICI treatment.

Abbreviations

BC = breast cancer; HR = hormone receptor; Body Mass Index = BMI; DM-BMI = DNA methylation based BMI index; TCGA = The Cancer Genome Atlas; GO = Gene Ontology; KEGG = Kyoto Encyclopedia of Genes and Genomes; ICI = immune checkpoint inhibitor; GEO = Gene Expression Omnibus; knn = k-nearest neighbors; SNPs = single nucleotide polymorphisms; TMB = Tumor mutation burden; Treg = regulatory T cells; IFNG = IFN- γ signature; IFNG.GS = IFNG hallmark gene set; TIDE = Tumor Immune Dysfunction and Exclusion; MDSCs = myeloid-derived suppressor cells; CAFs = cancer-associated fibroblasts; TAM-M2 = M2 subtype of tumor-associated macrophages; Chr = Chromosome; DMP = differentially methylated probes; GSEA = Gene Set Enrichment Analysis.

Declarations

Ethics approval and consent to participate

Not applicable

Consent for publication

Not applicable

Availability of data and material

Not applicable.

Competing interest

All the authors declare that they have no conflicts of interest.

Funding

Not applicable

Authors' contributions

XXM and KYN designed the overall project; XZC and YL analysed the data and wrote the manuscript; FJC and YL collected and analysed the data; XZC, LX and XXH did the statistical analysis. All the authors have read and approved the final manuscript.

Acknowledgements

Not applicable.

References

1. Shah SP, Roth A, Goya R, Oloumi A, Ha G, Zhao Y, Turashvili G, Ding J, Tse K, Haffari G, et al. The clonal and mutational evolution spectrum of primary triple-negative breast cancers. *Nature*. 2012;486(7403):395–9.
2. Bray F, Ferlay J, Soerjomataram I, Siegel RL, Torre LA, Jemal A. Global cancer statistics 2018: GLOBOCAN estimates of incidence and mortality worldwide for 36 cancers in 185 countries. *Cancer J Clin*. 2018;68(6):394–424.
3. Sung H, Siegel RL, Torre LA, Pearson-Stuttard J, Islami F, Fedewa SA, Goding Sauer A, Shuval K, Gapstur SM, Jacobs EJ, et al. Global patterns in excess body weight and the associated cancer burden. *Cancer J Clin*. 2019;69(2):88–112.
4. Picon-Ruiz M, Morata-Tarifa C, Valle-Goffin JJ, Friedman ER, Slingerland JM. Obesity and adverse breast cancer risk and outcome: Mechanistic insights and strategies for intervention. *Cancer J Clin*. 2017;67(5):378–97.

5. Copson ER, Cutress RI, Maishman T, Eccles BK, Gerty S, Stanton L, Altman DG, Durcan L, Wong C, Simmonds PD, et al. Obesity and the outcome of young breast cancer patients in the UK: the POSH study. *Annals of oncology: official journal of the European Society for Medical Oncology*. 2015;26(1):101–12.
6. Jiralerspong S, Goodwin PJ. Obesity and Breast Cancer Prognosis: Evidence, Challenges, and Opportunities. *Journal of clinical oncology: official journal of the American Society of Clinical Oncology*. 2016;34(35):4203–16.
7. Khandekar MJ, Cohen P, Spiegelman BM. Molecular mechanisms of cancer development in obesity. *Nature reviews Cancer*. 2011;11(12):886–95.
8. Prentice AM, Jebb SA. Beyond body mass index. *Obesity reviews: an official journal of the International Association for the Study of Obesity*. 2001;2(3):141–7.
9. Bosello O, Donataccio MP, Cuzzolaro M. Obesity or obesities? Controversies on the association between body mass index and premature mortality. *Eating weight disorders: EWD*. 2016;21(2):165–74.
10. Bray GA, Fruhbeck G, Ryan DH, Wilding JP. Management of obesity. *Lancet*. 2016;387(10031):1947–56.
11. Samblas M, Milagro FI, Martinez A. DNA methylation markers in obesity, metabolic syndrome, and weight loss. *Epigenetics*. 2019;14(5):421–44.
12. Ling C, Ronn T. Epigenetics in Human Obesity and Type 2 Diabetes. *Cell Metabol*. 2019;29(5):1028–44.
13. Hair BY, Xu Z, Kirk EL, Harlid S, Sandhu R, Robinson WR, Wu MC, Olshan AF, Conway K, Taylor JA, et al. Body mass index associated with genome-wide methylation in breast tissue. *Breast cancer research treatment*. 2015;151(2):453–63.
14. Hair BY, Troester MA, Edmiston SN, Parrish EA, Robinson WR, Wu MC, Olshan AF, Swift-Scanlan T, Conway K. Body mass index is associated with gene methylation in estrogen receptor-positive breast tumors. *Cancer epidemiology biomarkers prevention: a publication of the American Association for Cancer Research cosponsored by the American Society of Preventive Oncology*. 2015;24(3):580–6.
15. Chalmers ZR, Connelly CF, Fabrizio D, Gay L, Ali SM, Ennis R, Schrock A, Campbell B, Shlien A, Chmielecki J, et al. Analysis of 100,000 human cancer genomes reveals the landscape of tumor mutational burden. *Genome medicine*. 2017;9(1):34.
16. Yoshihara K, Shahmoradgoli M, Martinez E, Vegesna R, Kim H, Torres-Garcia W, Trevino V, Shen H, Laird PW, Levine DA, et al. Inferring tumour purity and stromal and immune cell admixture from expression data. *Nature communications*. 2013;4:2612.
17. Gentles AJ, Newman AM, Liu CL, Bratman SV, Feng W, Kim D, Nair VS, Xu Y, Khuong A, Hoang CD, et al. The prognostic landscape of genes and infiltrating immune cells across human cancers. *Nature medicine*. 2015;21(8):938–45.
18. Ayers M, Lunceford J, Nebozhyn M, Murphy E, Loboda A, Kaufman DR, Albright A, Cheng JD, Kang SP, Shankaran V, et al. IFN-gamma-related mRNA profile predicts clinical response to PD-1 blockade.

- J Clin Investig. 2017;127(8):2930–40.
19. Benci JL, Johnson LR, Choa R, Xu Y, Qiu J, Zhou Z, Xu B, Ye D, Nathanson KL, June CH, et al. Opposing Functions of Interferon Coordinate Adaptive and Innate Immune Responses to Cancer Immune Checkpoint Blockade. *Cell*. 2019;178(4):933–48 e914.
 20. Leone P, Shin EC, Perosa F, Vacca A, Dammacco F, Racanelli V. MHC class I antigen processing and presenting machinery: organization, function, and defects in tumor cells. *J Natl Cancer Inst*. 2013;105(16):1172–87.
 21. Jiang P, Gu S, Pan D, Fu J, Sahu A, Hu X, Li Z, Traugh N, Bu X, Li B, et al. Signatures of T cell dysfunction and exclusion predict cancer immunotherapy response. *Nature medicine*. 2018;24(10):1550–8.
 22. Joyce JA, Fearon DT. T cell exclusion, immune privilege, and the tumor microenvironment. *Science*. 2015;348(6230):74–80.
 23. Flaherty SE 3rd, Grijalva A, Xu X, Ables E, Nomani A, Ferrante AW Jr. A lipase-independent pathway of lipid release and immune modulation by adipocytes. *Science*. 2019;363(6430):989–93.
 24. von Boehmer H, Daniel C. Therapeutic opportunities for manipulating T(Reg) cells in autoimmunity and cancer. *Nature reviews Drug discovery*. 2013;12(1):51–63.
 25. Wang Z, Aguilar EG, Luna JI, Dunai C. **Paradoxical effects of obesity on T cell function during tumor progression and PD-1 checkpoint blockade**. 2019, 25(1):141–151.
 26. Lyman GH. Weight-based chemotherapy dosing in obese patients with cancer: back to the future. *Journal of oncology practice*. 2012;8(4):e62–4.
 27. Liedtke S, Schmidt ME, Vrieling A, Lukanova A, Becker S, Kaaks R, Zaineddin AK, Buck K, Benner A, Chang-Claude J, et al. Postmenopausal sex hormones in relation to body fat distribution. *Obesity (Silver Spring Md)*. 2012;20(5):1088–95.
 28. Karlsson AK, Kullberg J, Stokland E, Allvin K, Gronowitz E, Svensson PA, Dahlgren J. Measurements of total and regional body composition in preschool children: A comparison of MRI, DXA, and anthropometric data. *Obesity (Silver Spring Md)*. 2013;21(5):1018–24.
 29. Neamat-Allah J, Wald D, Hüsing A, Teucher B, Wendt A, Delorme S, Dinkel J, Vigl M, Bergmann MM, Feller S, et al. Validation of anthropometric indices of adiposity against whole-body magnetic resonance imaging—a study within the German European Prospective Investigation into Cancer and Nutrition (EPIC) cohorts. *PloS one*. 2014;9(3):e91586.
 30. Nimptsch K, Konigorski S, Pischon T. Diagnosis of obesity and use of obesity biomarkers in science and clinical medicine. *Metab Clin Exp*. 2019;92:61–70.
 31. Wahl S, Drong A, Lehne B, Loh M, Scott WR, Kunze S, Tsai PC, Ried JS, Zhang W, Yang Y, et al. Epigenome-wide association study of body mass index, and the adverse outcomes of adiposity. *Nature*. 2017;541(7635):81–6.

Figures

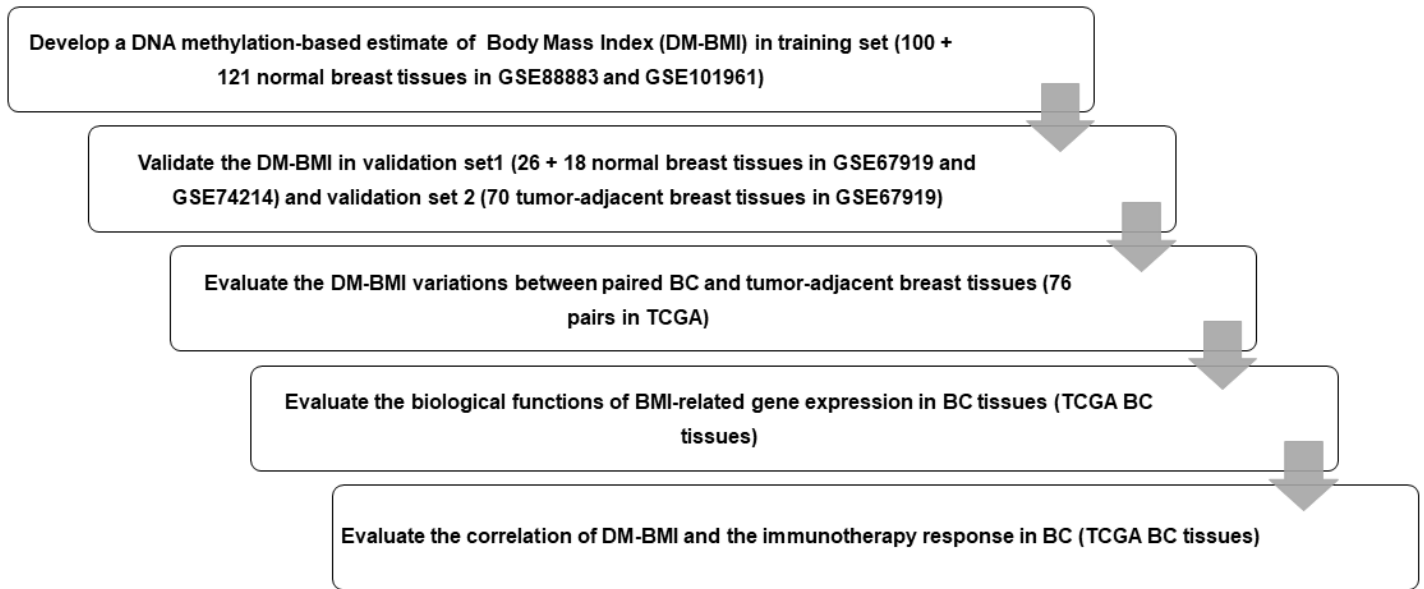


Figure 1

Flow chart of study design. We enrolled 221 normal breast tissues as training set to develop a lasso regression to predict DM-BMI and validated the accuracy of model with data of normal breast tissues and tumor-adjacent breast tissues. Then, we predict DM-BMI in 775 BC tissues and 76 matched tumor-adjacent breast tissues. The correlation between DM-BMI and clinical characteristics was assessed in BC tissues. Further, we identified the DM-BMI related gene profile and evaluated the relationships between DN-BMI and tumor immune response in BC tissues.

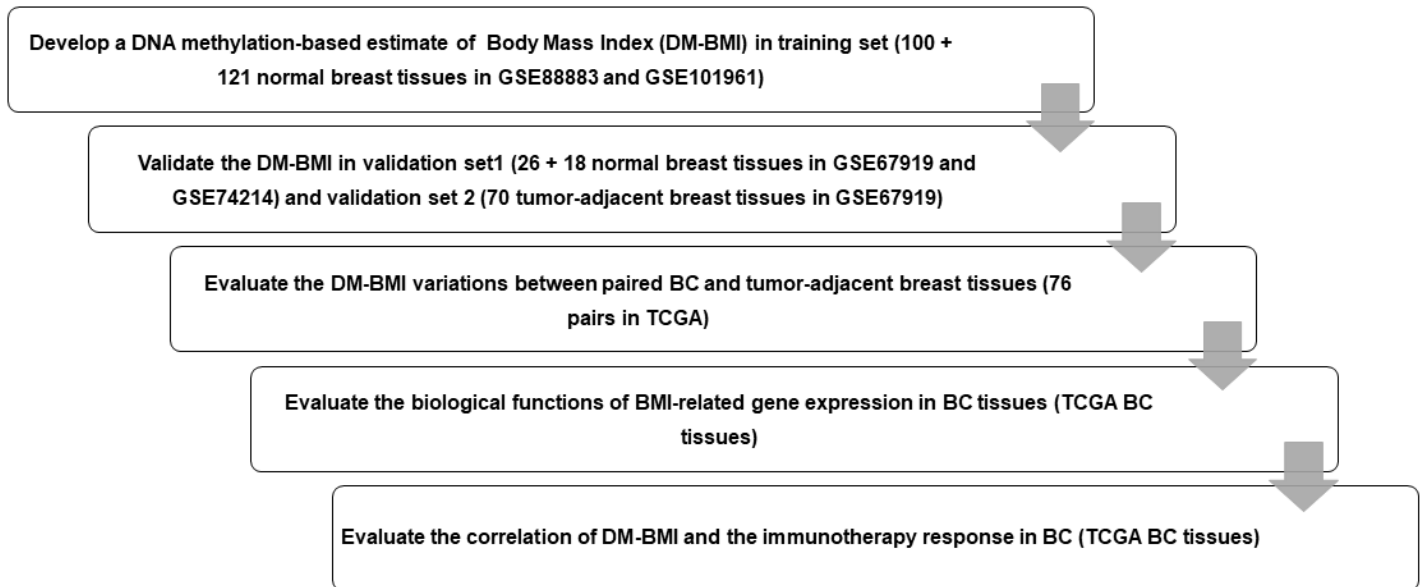


Figure 1

Flow chart of study design. We enrolled 221 normal breast tissues as training set to develop a lasso regression to predict DM-BMI and validated the accuracy of model with data of normal breast tissues and

tumor-adjacent breast tissues. Then, we predict DM-BMI in 775 BC tissues and 76 matched tumor-adjacent breast tissues. The correlation between DM-BMI and clinical characteristics was assessed in BC tissues. Further, we identified the DM-BMI related gene profile and evaluated the relationships between DN-BMI and tumor immune response in BC tissues.

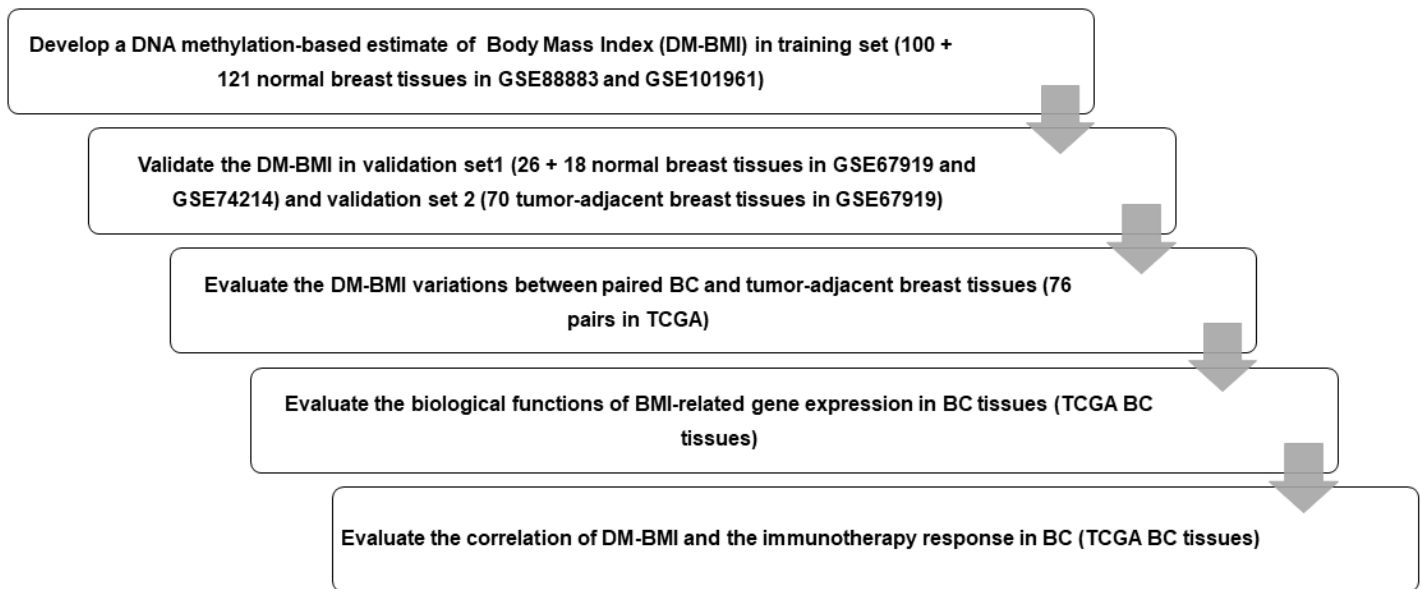


Figure 1

Flow chart of study design. We enrolled 221 normal breast tissues as training set to develop a lasso regression to predict DM-BMI and validated the accuracy of model with data of normal breast tissues and tumor-adjacent breast tissues. Then, we predict DM-BMI in 775 BC tissues and 76 matched tumor-adjacent breast tissues. The correlation between DM-BMI and clinical characteristics was assessed in BC tissues. Further, we identified the DM-BMI related gene profile and evaluated the relationships between DN-BMI and tumor immune response in BC tissues.

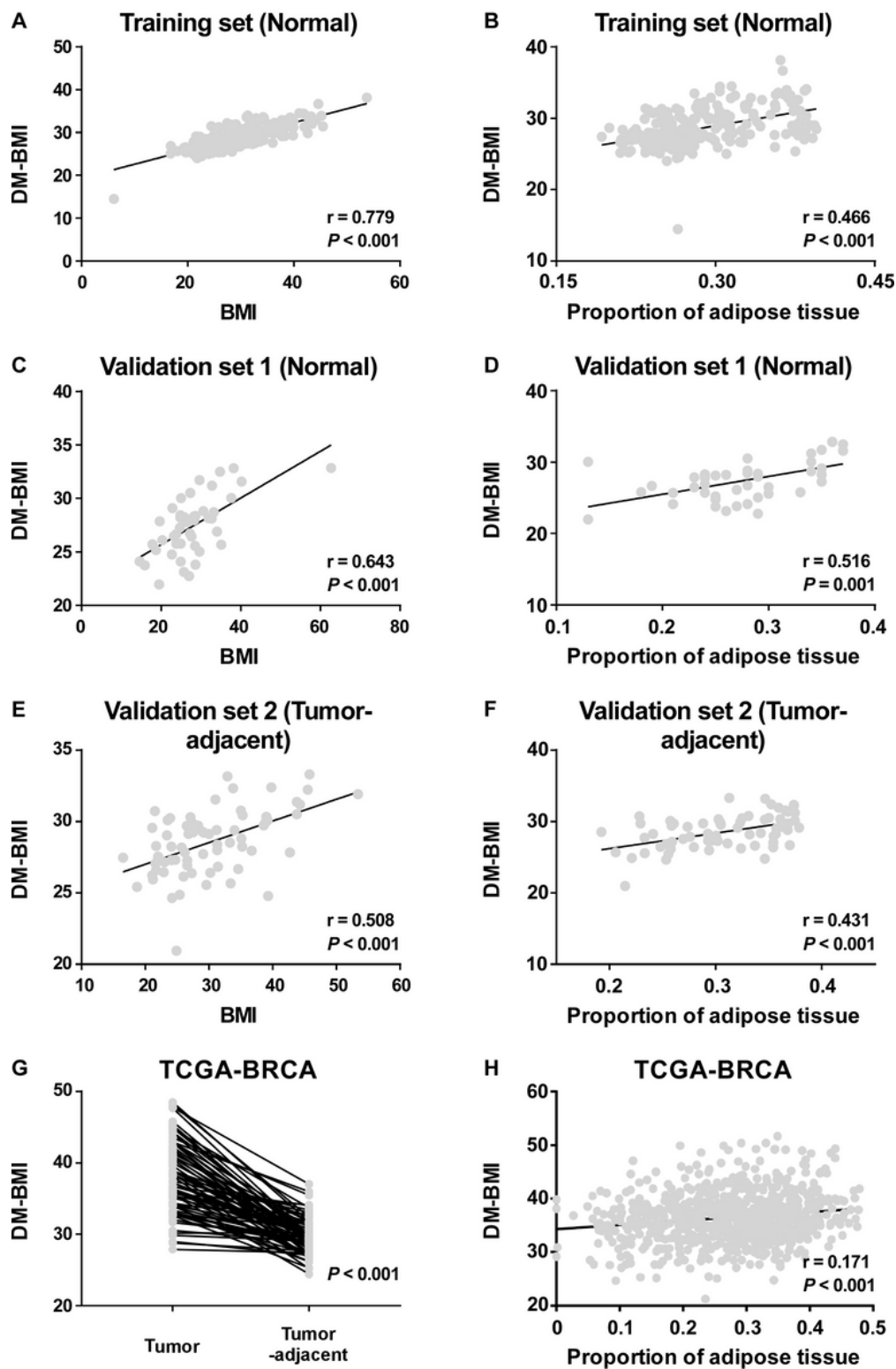


Figure 2

Development and validation of the DA-BMI predicting model. (A-B) Correlation of DM-BMI with (A) BMI and (B) proportion of adipose tissue in normal breast tissues based on the training set (GSE88883 and GSE101961). (C-D) Correlation of DM-BMI with (C) BMI and (D) proportion of adipose tissue in normal breast tissues based on the validation set1 (GSE67919 and GSE74214). (E-F) Correlation of DM-BMI with (E) BMI and (F) proportion of adipose tissue in tumor-adjacent breast tissues based on the validation set2

(GSE67919). (G) Analysing the differences of DM-BMI between tumor tissues (n = 76) and matched tumor-adjacent breast tissues (n = 76) based on TCGA-BRCA dataset. (H) Correlation of DM-BMI with proportion of adipose tissue in BC tissues based on TCGA-BRCA dataset (n = 775). For (A-F and H) r, Spearman correlation coefficient; for (G) P-values were determined by paired t-test.

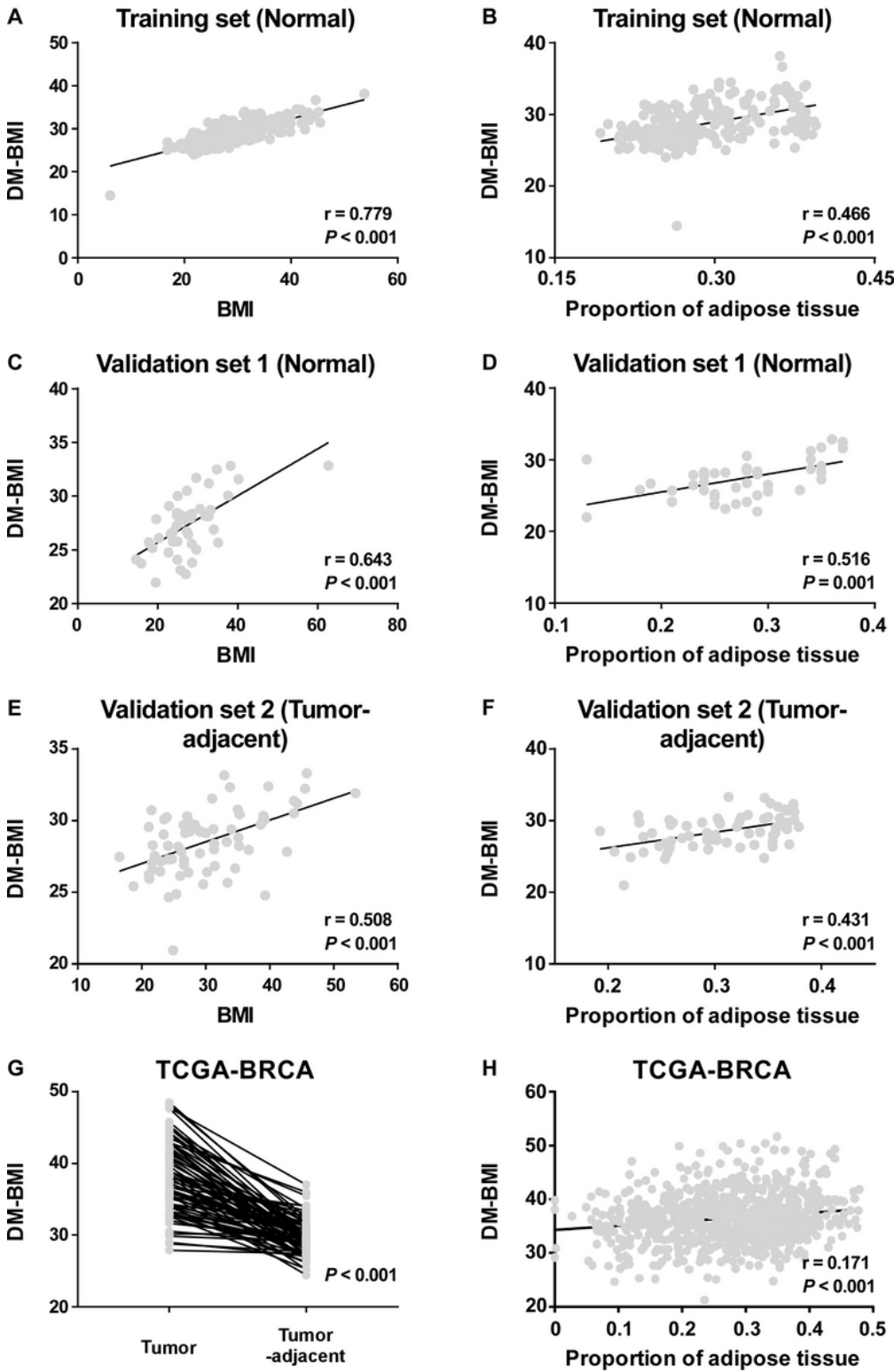


Figure 2

Development and validation of the DA-BMI predicting model. (A-B) Correlation of DM-BMI with (A) BMI and (B) proportion of adipose tissue in normal breast tissues based on the training set (GSE88883 and GSE101961). (C-D) Correlation of DM-BMI with (C) BMI and (D) proportion of adipose tissue in normal breast tissues based on the validation set1 (GSE67919 and GSE74214). (E-F) Correlation of DM-BMI with (E) BMI and (F) proportion of adipose tissue in tumor-adjacent breast tissues based on the validation set2 (GSE67919). (G) Analysing the differences of DM-BMI between tumor tissues (n = 76) and matched tumor-adjacent breast tissues (n = 76) based on TCGA-BRCA dataset. (H) Correlation of DM-BMI with proportion of adipose tissue in BC tissues based on TCGA-BRCA dataset (n = 775). For (A-F and H) r, Spearman correlation coefficient; for (G) P-values were determined by paired t-test.

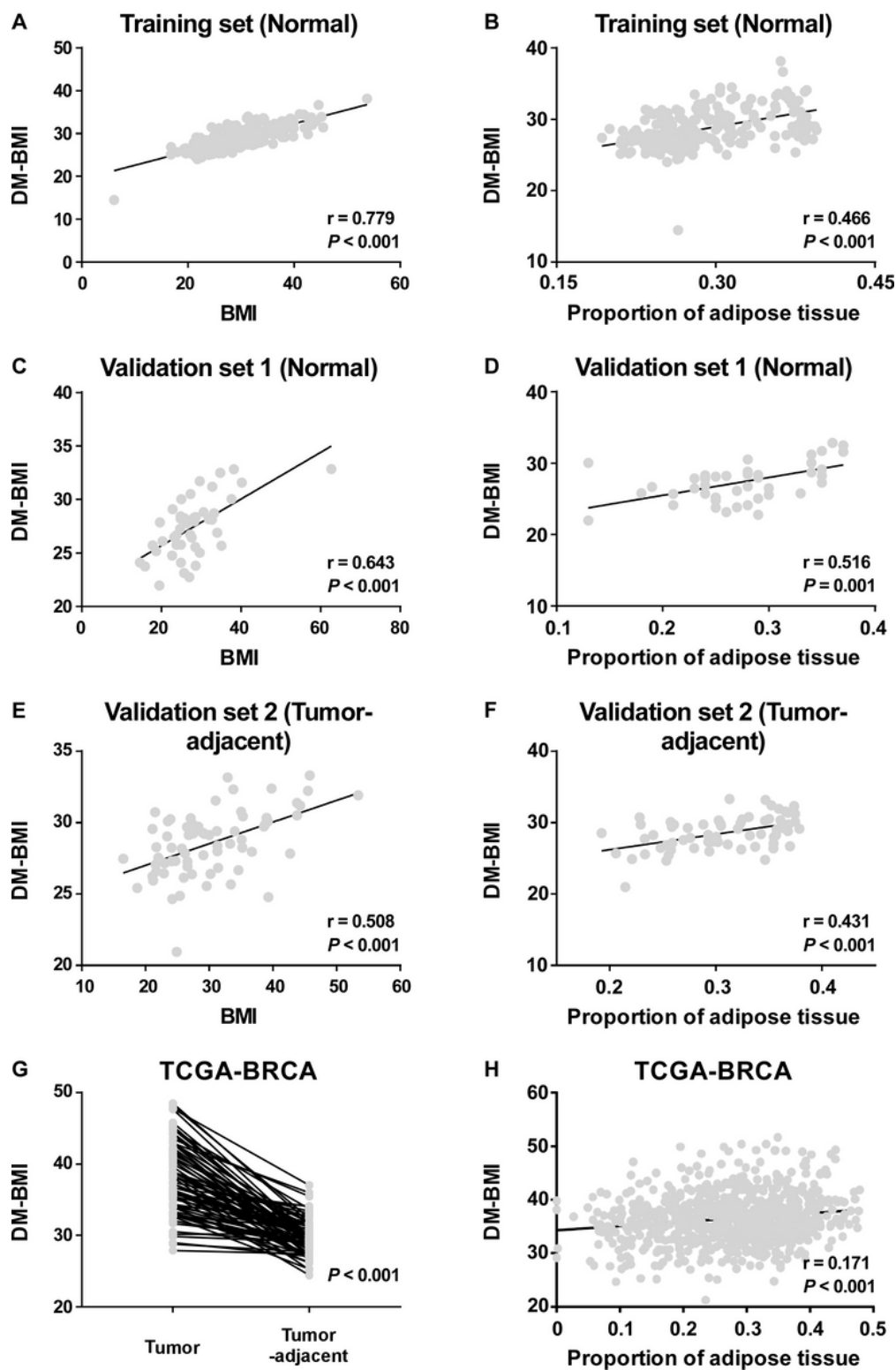


Figure 2

Development and validation of the DA-BMI predicting model. (A-B) Correlation of DM-BMI with (A) BMI and (B) proportion of adipose tissue in normal breast tissues based on the training set (GSE88883 and GSE101961). (C-D) Correlation of DM-BMI with (C) BMI and (D) proportion of adipose tissue in normal breast tissues based on the validation set1 (GSE67919 and GSE74214). (E-F) Correlation of DM-BMI with (E) BMI and (F) proportion of adipose tissue in tumor-adjacent breast tissues based on the validation set2

(GSE67919). (G) Analysing the differences of DM-BMI between tumor tissues (n = 76) and matched tumor-adjacent breast tissues (n = 76) based on TCGA-BRCA dataset. (H) Correlation of DM-BMI with proportion of adipose tissue in BC tissues based on TCGA-BRCA dataset (n = 775). For (A-F and H) r, Spearman correlation coefficient; for (G) P-values were determined by paired t-test.

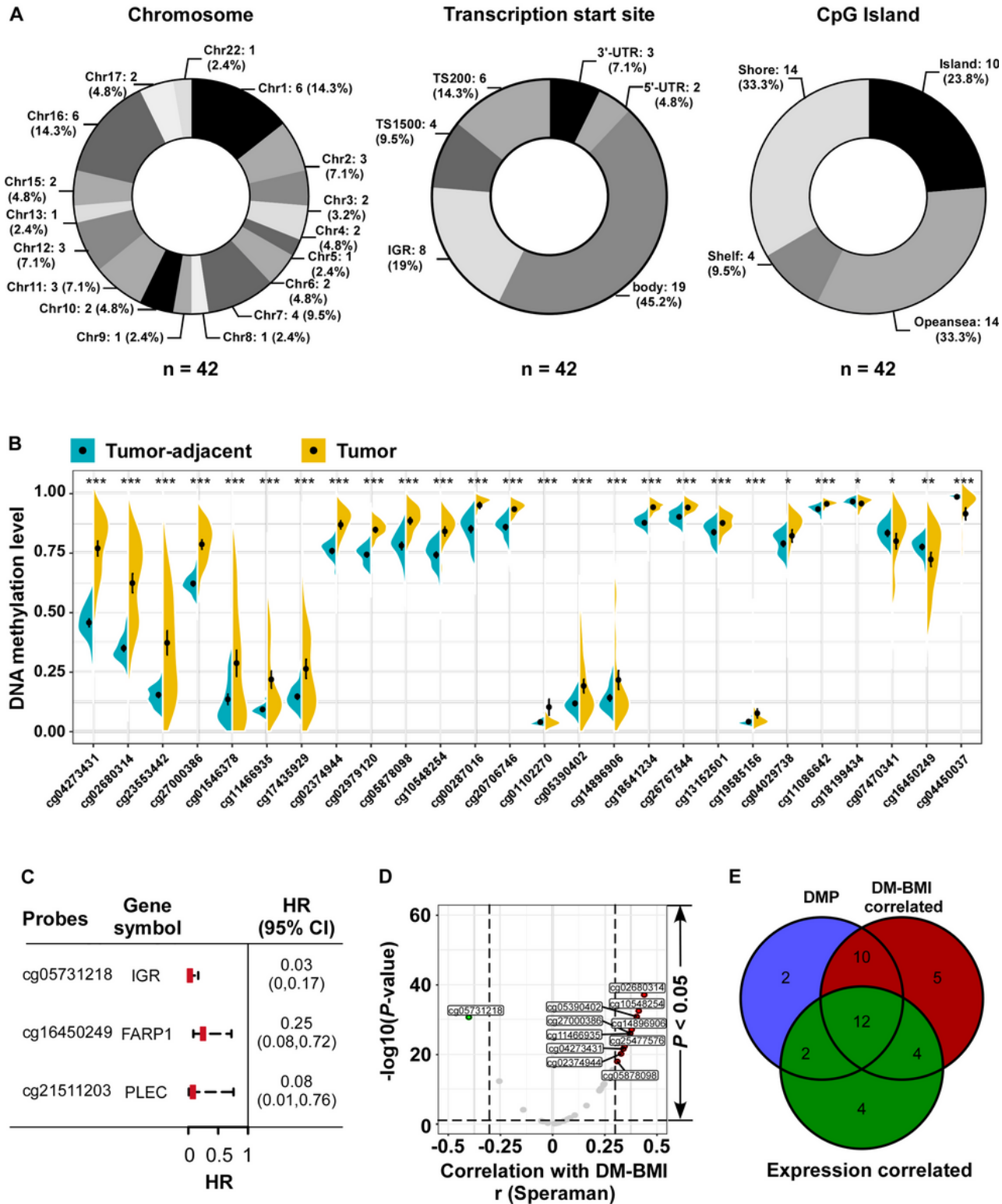


Figure 3

Characteristics analyses of BMI predictors. (A) Distribution of 42 BMI predictors referring to (Left) chromosome, (Middel) transcription Start Sites, CpG island were listed as number (proportion). For chromosome, no BMI predictors were located in Chr14, 18, 19, 20 and 21. (B) Identification of differential methylation BMI predictors between tumor tissues and matched tumor-adjacent breast tissues in TCGA dataset (n =76). * P <0.05, **P < 0.01, ***P < 0.001. (C) Forest plot of the prognostic related BMI predictors referring to DNA methylation level from TCGA BC tissues (n = 774): 3 BMI predictors (mapping to FARP1, PLEC, cg05731218 located in intergenic region/IGR) negatively correlated with overall survival. (D) Volcano plot of the correlation analysis between DM-BMI and methylation level of BMI predictors. r, Spearman correlation coefficient; 39 BMI predictors positively correlated with DM-BMI (BMI predictors with correlation coefficient > 0.3 were marked as red dot; n = 10), and 5 BMI predictors negatively correlated with DM-BMI (BMI predictors with Spearman correlation coefficient < -0.3 were marked as green dot; n = 1). E. Venn diagram of DMP, DM-BMI correlated and expression correlated BMI predictors. BMI predictors differentially methylated between tumor and tumor-adjacent tissues were labeled as blue; methylation level of BMI predictors correlated with DM-BMI were labeled as red; methylation level of BMI predictors negatively correlated with gene expression were labeled as green.

referring to DNA methylation level from TCGA BC tissues (n = 774): 3 BMI predictors (mapping to FARP1, PLEC, cg05731218 located in intergenic region/IGR) negatively correlated with overall survival. (D) Volcano plot of the correlation analysis between DM-BMI and methylation level of BMI predictors. r, Spearman correlation coefficient; 39 BMI predictors positively correlated with DM-BMI (BMI predictors with correlation coefficient > 0.3 were marked as red dot; n = 10), and 5 BMI predictors negatively correlated with DM-BMI (BMI predictors with Spearman correlation coefficient < -0.3 were marked as green dot; n = 1). E. Venn diagram of DMP, DM-BMI correlated and expression correlated BMI predictors. BMI predictors differentially methylated between tumor and tumor-adjacent tissues were labeled as blue; methylation level of BMI predictors correlated with DM-BMI were labeled as red; methylation level of BMI predictors negatively correlated with gene expression were labeled as green.

referring to DNA methylation level from TCGA BC tissues (n = 774): 3 BMI predictors (mapping to FARP1, PLEC, cg05731218 located in intergenic region/IGR) negatively correlated with overall survival. (D) Volcano plot of the correlation analysis between DM-BMI and methylation level of BMI predictors. r, Spearman correlation coefficient; 39 BMI predictors positively correlated with DM-BMI (BMI predictors with correlation coefficient > 0.3 were marked as red dot; n = 10), and 5 BMI predictors negatively correlated with DM-BMI (BMI predictors with Spearman correlation coefficient < -0.3 were marked as green dot; n = 1). E. Venn diagram of DMP, DM-BMI correlated and expression correlated BMI predictors. BMI predictors differentially methylated between tumor and tumor-adjacent tissues were labeled as blue; methylation level of BMI predictors correlated with DM-BMI were labeled as red; methylation level of BMI predictors negatively correlated with gene expression were labeled as green.

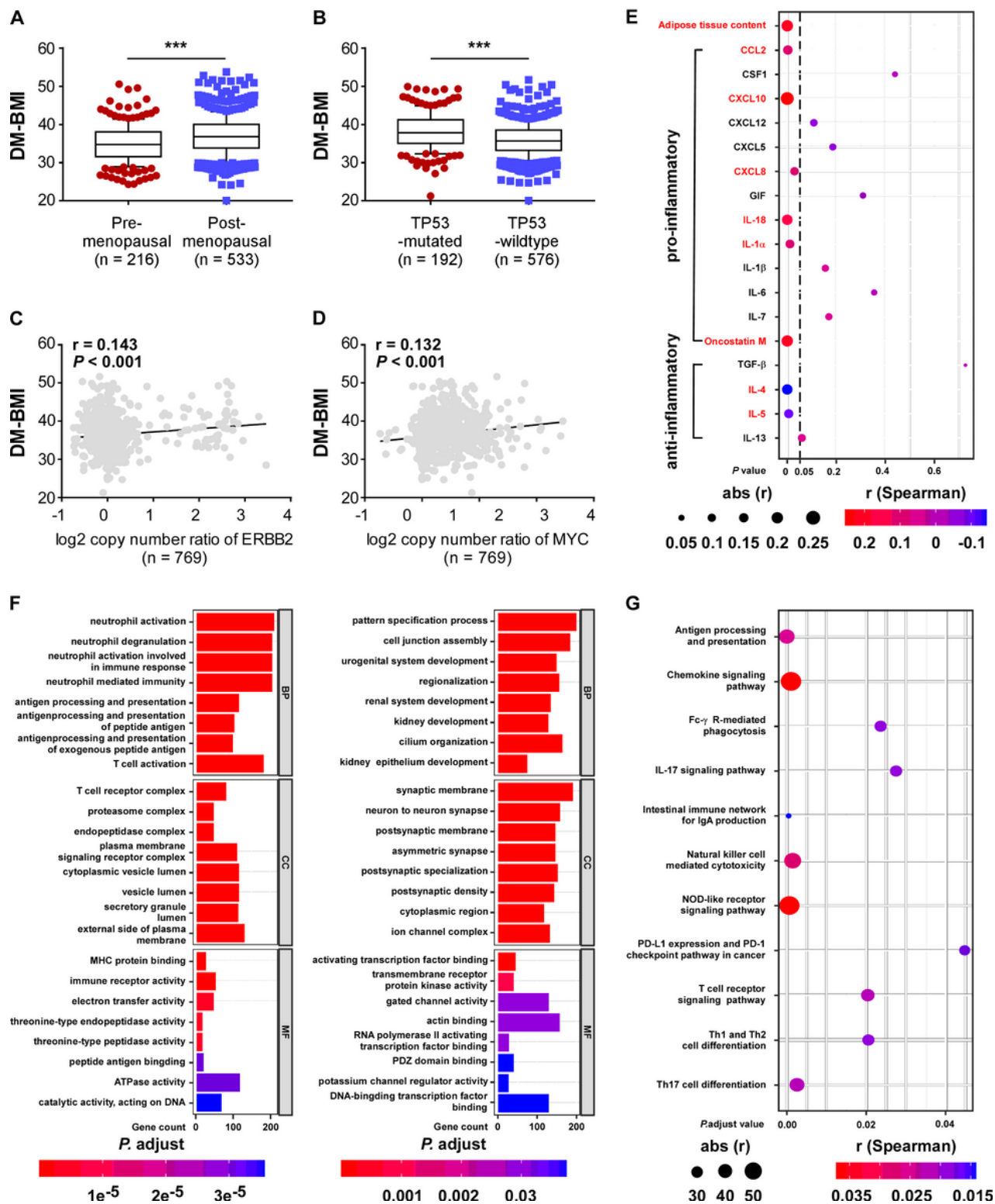


Figure 4

Functional and clinical characteristics analysis of DM-BMI related gene profile in BC. (A-B) Analysing the differences of DM-BMI based on (A) menopause status of patients (n = 749) or TP53 mutation status (n = 768) based on TCGA-BRCA dataset. (C-D) Correlation of DM-BMI with copy number of (C) ERBB2 and (D) MYC. r, Spearman correlation coefficient. (E) Correlation of DM-BMI and expression of pro/anti-inflammatory adipokines in BC tissues (n = 771). Expression of adipokines significantly correlated with

DM-BMI were labeled as red. (F) GO function analysis of DM-BMI related gene. (Left) Analysis of gene whose mRNA expression positively correlated with DM-BMI; [18] analysis of gene whose mRNA expression negatively correlated with DM-BMI. (G) Analysis of DM-BMI related gene enrichment in immunologic pathway based on KEGG database. Gene ratio was defined as: number of gene enriched to target pathway/number of DM-BMI related gene included in the KEGG dataset.

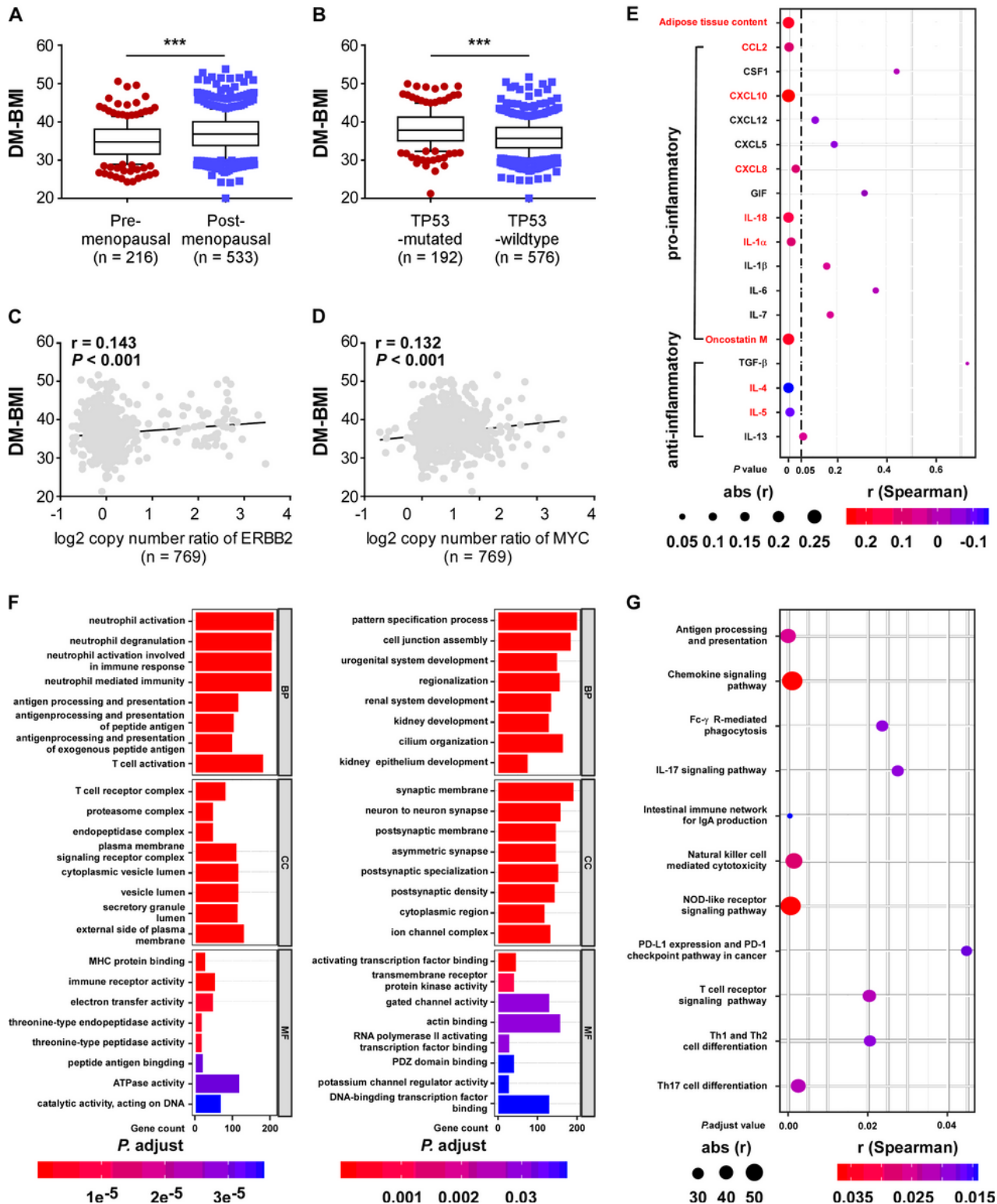


Figure 4

Functional and clinical characteristics analysis of DM-BMI related gene profile in BC. (A-B) Analysing the differences of DM-BMI based on (A) menopause status of patients (n = 749) or TP53 mutation status (n = 768) based on TCGA-BRCA dataset. (C-D) Correlation of DM-BMI with copy number of (C) ERBB2 and (D) MYC. r, Spearman correlation coefficient. (E) Correlation of DM-BMI and expression of pro/anti-inflammatory adipokines in BC tissues (n = 771). Expression of adipokines significantly correlated with DM-BMI were labeled as red. (F) GO function analysis of DM-BMI related gene. (Left) Analysis of gene whose mRNA expression positively correlated with DM-BMI; [18] analysis of gene whose mRNA expression negatively correlated with DM-BMI. (G) Analysis of DM-BMI related gene enrichment in immunologic pathway based on KEGG database. Gene ratio was defined as: number of gene enriched to target pathway/number of DM-BMI related gene included in the KEGG dataset.

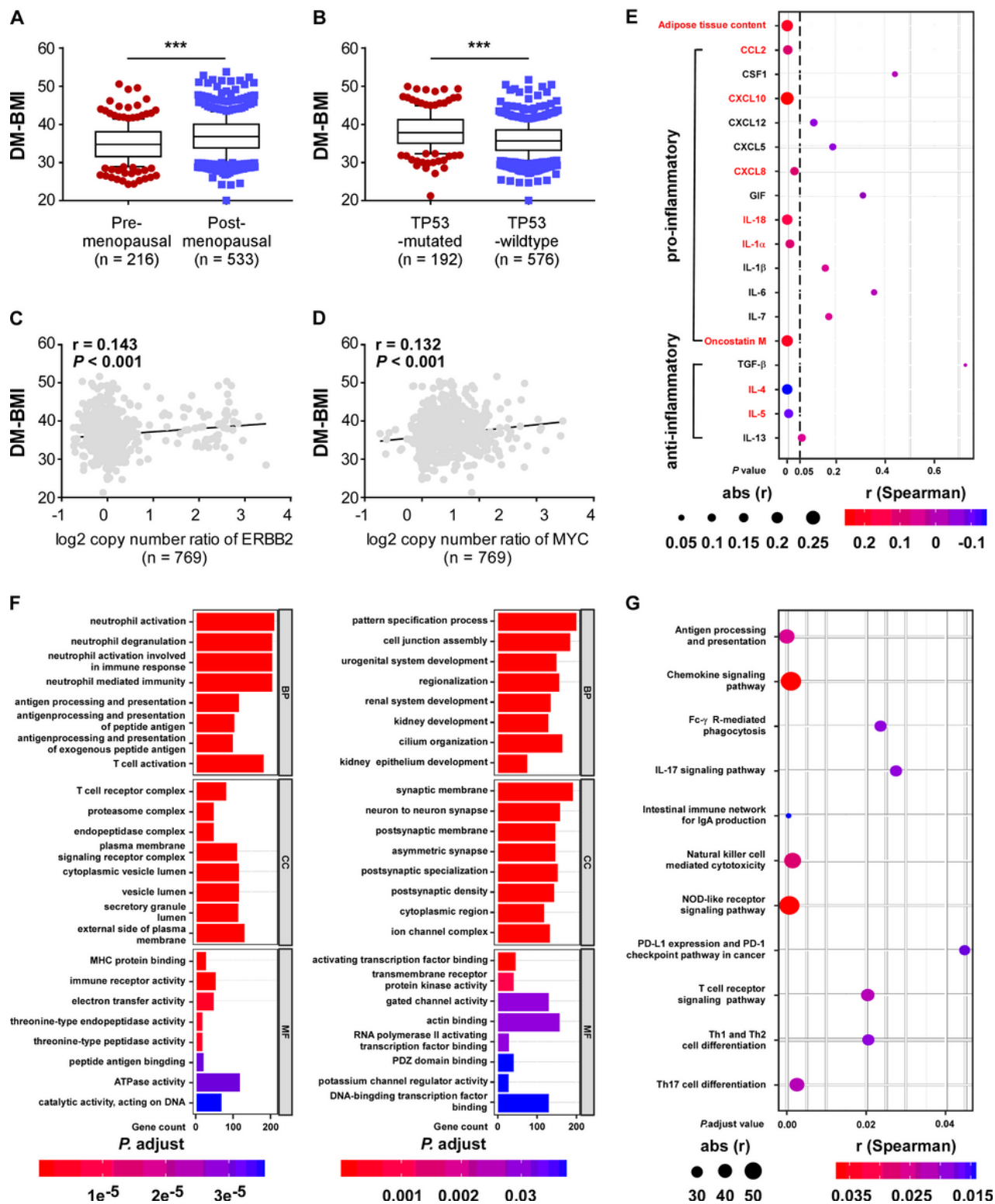


Figure 4

Functional and clinical characteristics analysis of DM-BMI related gene profile in BC. (A-B) Analysing the differences of DM-BMI based on (A) menopause status of patients (n = 749) or TP53 mutation status (n = 768) based on TCGA-BRCA dataset. (C-D) Correlation of DM-BMI with copy number of (C) ERBB2 and (D) MYC. r, Spearman correlation coefficient. (E) Correlation of DM-BMI and expression of pro/anti-inflammatory adipokines in BC tissues (n = 771). Expression of adipokines significantly correlated with

DM-BMI were labeled as red. (F) GO function analysis of DM-BMI related gene. (Left) Analysis of gene whose mRNA expression positively correlated with DM-BMI; [18] analysis of gene whose mRNA expression negatively correlated with DM-BMI. (G) Analysis of DM-BMI related gene enrichment in immunologic pathway based on KEGG database. Gene ratio was defined as: number of gene enriched to target pathway/number of DM-BMI related gene included in the KEGG dataset.

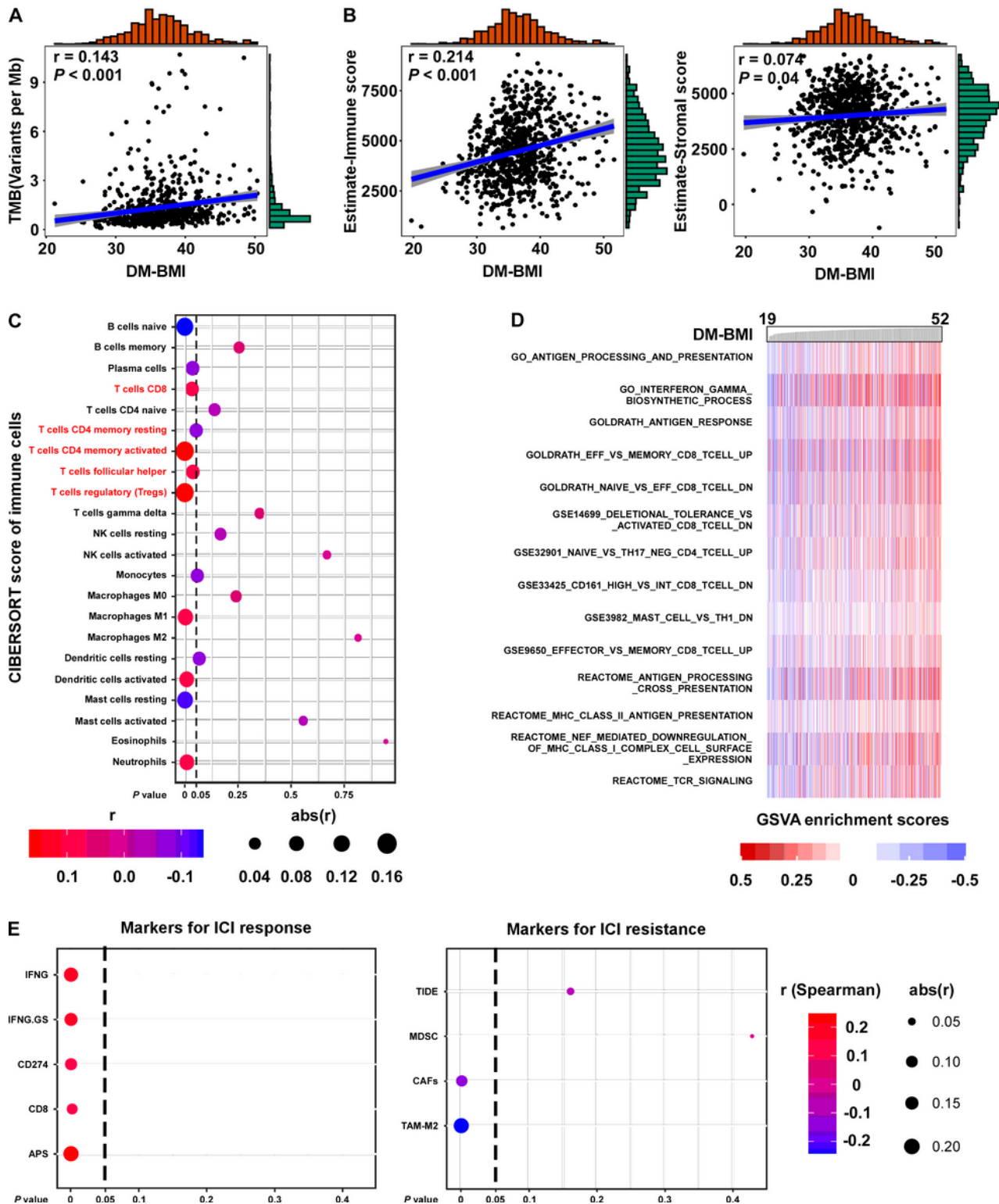


Figure 5

DM-BMI correlated with T cell infiltration and ICI response in BC. (A) Correlation of DM-BMI with tumor mutation burden (TMB) in BC tissues (TCGA-BRCA, n = 775). Numerical distribution of DM-BMI and TMB were shown on the above x and the right y axis, respectively. (B) Correlation of DM-BMI with the level of infiltrating immune cells (Left, estimate-immune score) and the level of stromal cells (Right, estimate-stromal score) in BC tissues (TCGA-BRCA, n = 772). Numerical distribution of DM-BMI and estimate-immune/stromal score were shown on the above x and the right y axis, respectively. (C) Correlation of DM-BMI with 22 type of immune cell components was shown by dotplot. 5 of 7 T cell content correlated with DM-BMI which were labeled in red. (D) GSVA analysis identified immunologic pathway which positively correlated DM-BMI. Enrichment scores of pathways from GSEA-Molecular Signatures Database were calculated using GSVA in BC tissues (TCGA-BRCA-mRNA data, n = 771). Immunologic gene sets which significantly correlated with DM-BMI were displayed ($r > 0.3$). (E) Correlation of DM-BMI with markers for ICI response/resistance was shown by dotplot. For (A-B), r , Spearman correlation coefficient.

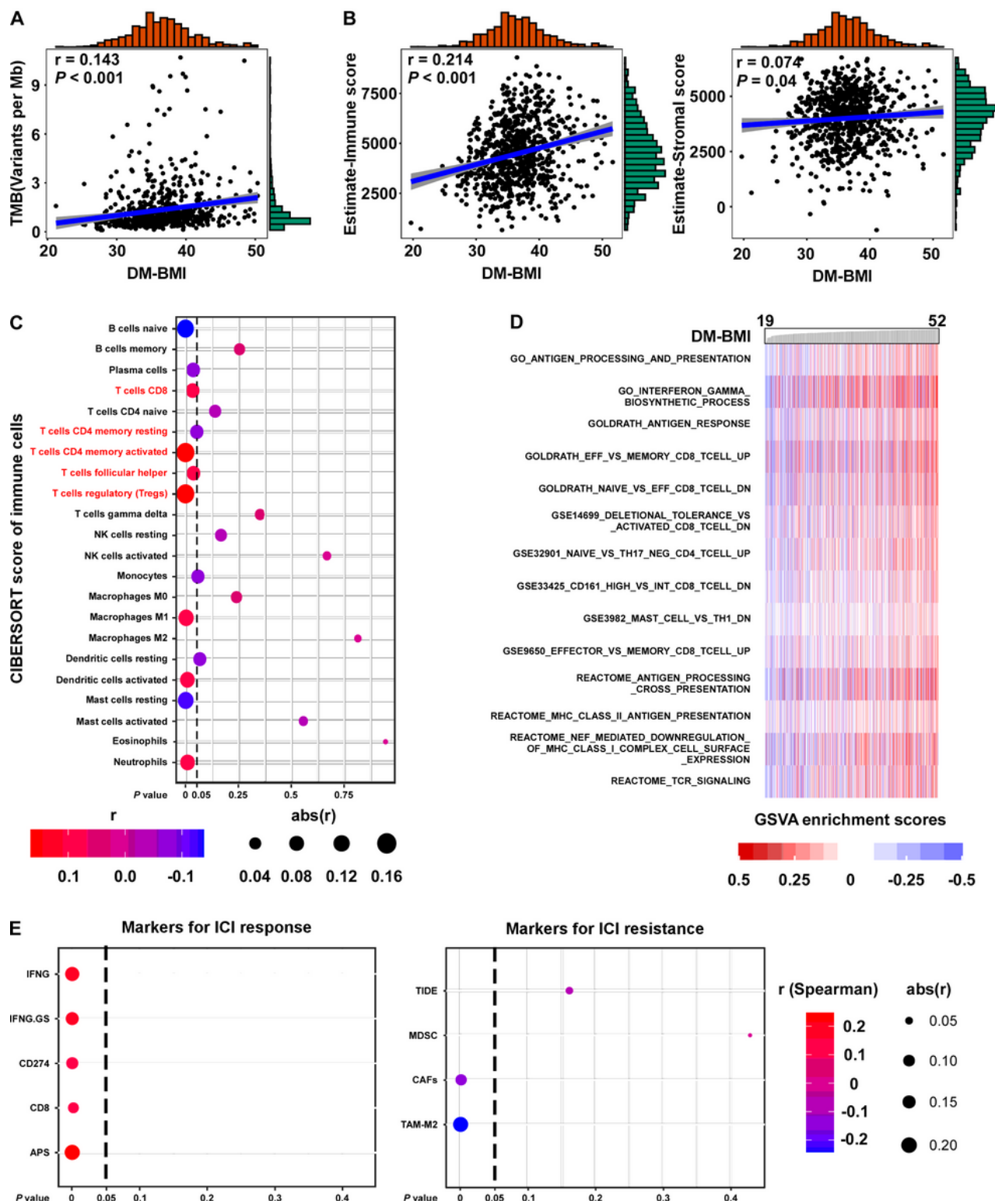


Figure 5

DM-BMI correlated with T cell infiltration and ICI response in BC. (A) Correlation of DM-BMI with tumor mutation burden (TMB) in BC tissues (TCGA-BRCA, $n = 775$). Numerical distribution of DM-BMI and TMB were shown on the above x and the right y axis, respectively. (B) Correlation of DM-BMI with the level of infiltrating immune cells (Left, estimate-immune score) and the level of stromal cells (Right, estimate-stromal score) in BC tissues (TCGA-BRCA, $n = 772$). Numerical distribution of DM-BMI and estimate-

immune/stromal score were shown on the above x and the right y axis, respectively. (C) Correlation of DM-BMI with 22 type of immune cell components was shown by dotplot. 5 of 7 T cell content correlated with DM-BMI which were labeled in red. (D) GSEA analysis identified immunologic pathway which positively correlated DM-BMI. Enrichment scores of pathways from GSEA-Molecular Signatures Database were calculated using GSVA in BC tissues (TCGA-BRCA-mRNA data, n = 771). Immunologic gene sets which significantly correlated with DM-BMI were displayed ($r > 0.3$). (E) Correlation of DM-BMI with markers for ICI response/resistance was shown by dotplot. For (A-B), r , Spearman correlation coefficient.

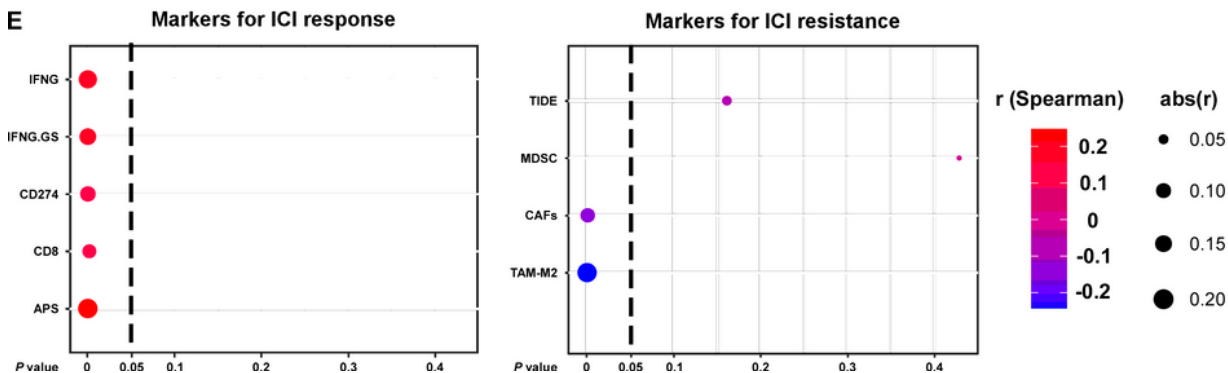
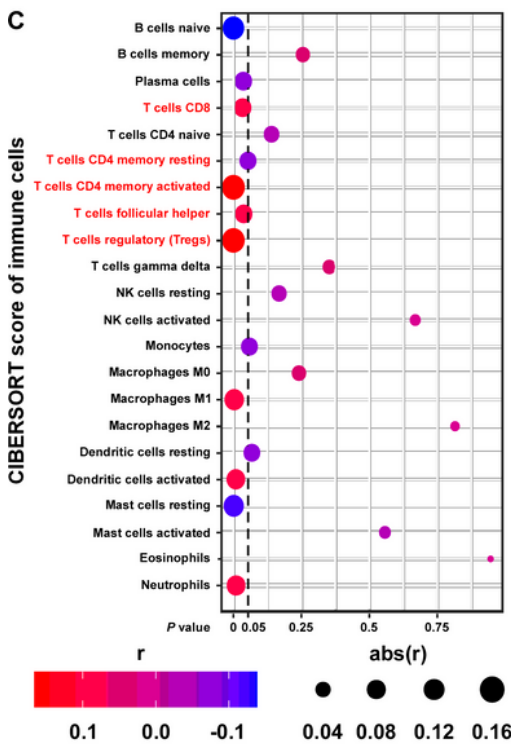
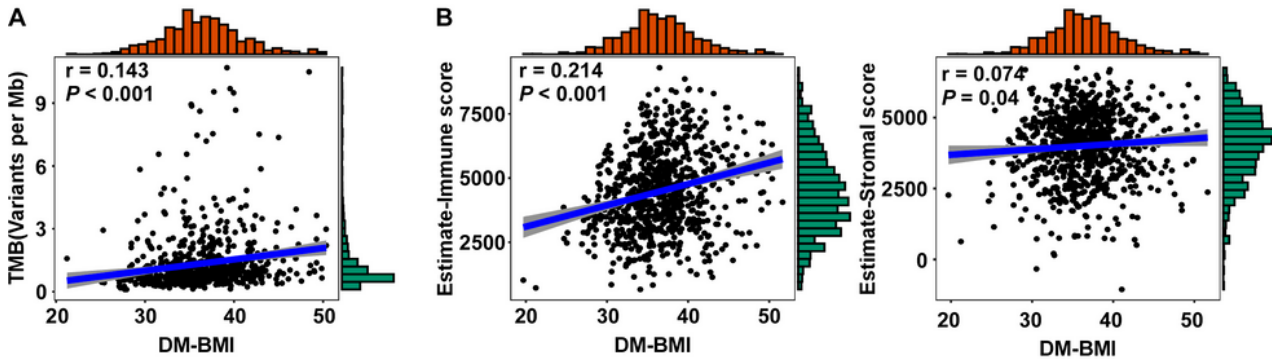


Figure 5

DM-BMI correlated with T cell infiltration and ICI response in BC. (A) Correlation of DM-BMI with tumor mutation burden (TMB) in BC tissues (TCGA-BRCA, n = 775). Numerical distribution of DM-BMI and TMB were shown on the above x and the right y axis, respectively. (B) Correlation of DM-BMI with the level of infiltrating immune cells (Left, estimate-immune score) and the level of stromal cells (Right, estimate-stromal score) in BC tissues (TCGA-BRCA, n = 772). Numerical distribution of DM-BMI and estimate-immune/stromal score were shown on the above x and the right y axis, respectively. (C) Correlation of DM-BMI with 22 type of immune cell components was shown by dotplot. 5 of 7 T cell content correlated with DM-BMI which were labeled in red. (D) GSEA analysis identified immunologic pathway which positively correlated DM-BMI. Enrichment scores of pathways from GSEA-Molecular Signatures Database were calculated using GSEA in BC tissues (TCGA-BRCA-mRNA data, n = 771). Immunologic gene sets which significantly correlated with DM-BMI were displayed ($r > 0.3$). (E) Correlation of DM-BMI with markers for ICI response/resistance was shown by dotplot. For (A-B), r , Spearman correlation coefficient.

Supplementary Files

This is a list of supplementary files associated with this preprint. Click to download.

- [Supplementarymaterial1DMBMIandBMIdata.xls](#)
- [Supplementarymaterial1DMBMIandBMIdata.xls](#)
- [Supplementarymaterial1DMBMIandBMIdata.xls](#)
- [Supplementarymaterial2DMBMIofTCGAcases.xls](#)
- [Supplementarymaterial2DMBMIofTCGAcases.xls](#)
- [Supplementarymaterial2DMBMIofTCGAcases.xls](#)
- [Supplementarymaterial3adiposetissuecontent.xls](#)
- [Supplementarymaterial3adiposetissuecontent.xls](#)
- [Supplementarymaterial3adiposetissuecontent.xls](#)
- [Supplementarymaterial4phenotypeofTCGA.xls](#)
- [Supplementarymaterial4phenotypeofTCGA.xls](#)
- [Supplementarymaterial4phenotypeofTCGA.xls](#)
- [Supplementarymaterial5coefficientsofBMIpredictors.xls](#)
- [Supplementarymaterial5coefficientsofBMIpredictors.xls](#)
- [Supplementarymaterial5coefficientsofBMIpredictors.xls](#)
- [Supplementtitlesandlegendstofigures.docx](#)
- [Supplementtitlesandlegendstofigures.docx](#)
- [Supplementtitlesandlegendstofigures.docx](#)